Sensitivities to feebly interacting particles: public and unified calculations

Maksym Ovchynnikov,[a,b] **Jean-Loup Tastet,**[c] **Oleksii Mikulenko,**[b]
Kyrylo Bondarenko[d,e,f]

[a]*Institut für Astroteilchen Physik, Karlsruher Institut für Technologie (KIT), Hermann-von-Helmholtz-Platz 1, 76344 Eggenstein-Leopoldshafen, Germany*

[b]*Instituut-Lorentz, Leiden University, Niels Bohrweg 2, 2333 CA Leiden, The Netherlands*

[c]*Departamento de Física Teórica and Instituto de Física Teórica UAM/CSIC, Universidad Autónoma de Madrid, Cantoblanco, 28049, Madrid, Spain*

[d]*IFPU, Institute for Fundamental Physics of the Universe, via Beirut 2, I-34014 Trieste, Italy*

[e]*SISSA, via Bonomea 265, I-34132 Trieste, Italy*

[f]*INFN, Sezione di Trieste, SISSA, Via Bonomea 265, 34136, Trieste, Italy*

E-mail: maksym.ovchynnikov@kit.edu, jean-loup.tastet@uam.es, oleksii.mikulenko@lorentz.leidenuniv.nl, kyrylo.bondarenko@sissa.it

ABSTRACT: The idea that new physics could take the form of feebly interacting particles (FIPs) — particles with a mass below the electroweak scale, but which may have evaded detection due to their tiny couplings or very long lifetime — has gained a lot of traction in the last decade, and numerous experiments have been proposed to search for such particles. It is important, and now very timely, to consistently compare the potential of these experiments for exploring the parameter space of various well-motivated FIPs. The present paper addresses this pressing issue by presenting an open-source tool to estimate the sensitivity of many experiments — located at Fermilab or at the CERN's SPS, LHC, and FCC-hh — to various models of FIPs in a unified way: the `Mathematica`-based code `SensCalc`.

Contents

1 Introduction

The well-known shortcomings of the Standard Model suggest to us the existence of new physics "Beyond the Standard Model" (BSM), that is generally expected to involve new particles. There is currently no clear theoretical guidance, nor experimental hints, about the mass of the hypothetical new particles, which could range from sub-eV all the way up to the Planck scale. Particles with a mass below the electroweak scale are of particular interest experimentally, since they may be numerously produced at accelerators. Past experiments have already excluded the largest values of the couplings for such particles; hence they are called *feebly interacting particles*, or *FIPs* for short. FIPs may be searched for both at the main detectors of colliders (ATLAS, CMS and LHCb at the LHC, or their equivalents at future colliders such as the FCC-hh) which are located very close to the collision point, or at so-called *lifetime-frontier* experiments, which re-use existing facilities or infrastructure and place a displaced decay volume near an interaction point or target. Lifetime-frontier

experiments may be broadly split into two classes [1]: collider-based, which consist of a decay volume placed near the interaction points of ATLAS, CMS, and LHCb, and extracted-beam experiments, which use an extracted beam line hitting a target.

During the last few years, many lifetime-frontier experiments have been proposed. Among extracted-beam experiments, we can list SHiP [2, 3], SHADOWS [4], and HIKE [5] at the SPS, and DUNE [6, 7] and DarkQuest [8] at Fermilab. The proposed LHC-based experiments include MATHUSLA [9] and FACET [10], associated with CMS; FASER [11], SND@LHC [12] (together with their upgrades, AdvSND and FASER2) and ANUBIS [13], close to the ATLAS interaction point; Codex-b [14] near LHCb; and AL3X [15] at ALICE. Furthermore, lifetime-frontier experiments will likely remain part of the physics program of future colliders, such as the FCC-hh [16].

In order to evaluate the potential of those experiments to search for generic FIPs, the PBC initiative has proposed [1] a few benchmark models. They include dark photons, millicharged particles, dark scalars, heavy neutral leptons, and axion-like particles coupled to various SM particles.

While some of the experiments from the above list are already running, many are still at the status of proposals. Their design is not finalized yet, and is still undergoing optimization. Their sensitivity can be optimized by focusing on two key aspects: increasing the rate of events that contain FIPs, and reducing the Standard Model (SM) backgrounds. Studying the background requires knowing the detailed specifications of the experimental setup, background-reducing systems, and surrounding infrastructure. As a result, full simulations are required, which accurately trace each event starting from the initial proton collision and ending with the interactions of the background particles with the detector material. Most of the experimental proposals claim to achieve zero background level. In contrast, the evaluation of the FIP event rate is comparatively less affected by these complexities. This is the case, in particular, when the FIPs are produced at the collision point. They would then propagate through the infrastructure without being affected (due to their tiny interaction strength), and decay or scatter inside the decay volume with some tiny probability. If the reaction products reach the detector and satisfy some simple kinematic cuts, they could typically be detected with ≈ 1 efficiency. Therefore, the sensitivity[1] of a given experiment to FIPs is determined mainly by 1) the distribution of FIPs at the

---

[1]When talking about "sensitivity", it is important to point out the distinction between "exclusion" sensitivity (rejecting the New Physics hypothesis in the absence of signal) and "discovery" sensitivity (rejecting the Standard Model in favor of New Physics if a signal is observed). While the former is not very sensitive to the exact background expectation as long as it is $\lesssim 1$, the latter strongly depends on it. Throughout this paper, we mean "exclusion sensitivity" whenever we use the word "sensitivity" unqualified. However, we advise the reader to keep this distinction in mind when comparing the physics potential of various experiments: indeed, two experiments with the same exclusion sensitivity could in principle have significantly different discovery sensitivities.

facility housing the experiment and 2) the geometry of the experiment itself.

Despite the relative simplicity of estimating the sensitivity to FIPs, there exists a caveat that can make their comparison challenging: the sensitivity estimates performed by the various experimental collaborations are not publicly accessible. This is crucial for three reasons. First, there is often no unique description of the production and decay of a given FIP in the literature. This is related to either theoretical uncertainties in the description of the FIP phenomenology, or different conventions in the definition of the model. As a result, different collaborations can end up using different FIP descriptions; sometimes, even the definition of the FIP coupling is different (see Appendix A). Secondly, due to the rapid pace of change as the experiment's design is being optimized, there may exist a mismatch between, on the one hand, the experimental setup and/or the assumptions used and, on the other hand, the reported sensitivity, even within a same document (see Fig. 4 and the corresponding discussion). Indeed, in order to update the sensitivity while the setup is undergoing optimization, collaborations would need to re-launch full-scale simulations, which require a lot of time, computational resources and person-power. Finally, these calculations are black-box: they do not provide a qualitative understanding of the sensitivity. This problem becomes especially important when comparing the sensitivities of various experiments to understand which one is better suited to probe a given region of the FIP parameter space.

To address these issues, a public tool that can calculate the sensitivity of various experiments to FIPs — in a unified and transparent way — is required. Several publicly available packages can already perform such sensitivity calculations [17, 18]. However, they are limited to a specific type of facilities: either beam dump experiments or colliders. This paper presents the `Mathematica` [19] code `SensCalc` [20], that can evaluate the sensitivity of the various experiments proposed at LBNE, SPS, LHC, and FCC-hh to various FIPs.[2] The code is based on a semi-analytic approach developed in Ref. [21] and further improved and cross-checked in Refs. [16, 22, 23] (see also [24, 25]), where the number of events is approximated by the integral of several quantities: the FIP angle-energy distribution, its decay probability, the geometric acceptance of FIPs, and the acceptance of its decay products. Most of these quantities can be accurately computed analytically, which is especially attractive as it improves the transparency of the computations.

The present paper is organized as follows. In Sec. 2, we discuss the semi-analytic method that we use for calculating the sensitivity, together with its validation and limitations. In Sec. 3, we provide a brief description of `SensCalc`, specifying the list of currently implemented experiments and models of FIPs. We also compare it with other publicly available packages for computing the sensitivity, as well as with `SensMC` [26], a simplified Monte-Carlo simulation that we have specifically developed

---

[2]Available at https://doi.org/10.5281/zenodo.7957785 .

to validate `SensCalc`. Finally, we conclude in Sec. 4.

2 Semi-analytic approach to calculate sensitivities

2.1 Method

This work concentrates on FIPs produced at the collision point (or close to it). In this case, the production is unaffected by the surrounding infrastructure. We calculate the number of events involving a decaying FIP using the following expression:

$$N_{\text{ev}} = \sum_i N_{\text{prod}}^{(i)} \int dE d\theta dz \ f^{(i)}(\theta, E) \cdot \epsilon_{\text{az}}(\theta, z) \cdot \frac{dP_{\text{dec}}}{dz} \cdot \epsilon_{\text{dec}}(m, \theta, E, z) \cdot \epsilon_{\text{rec}} \quad (2.1)$$
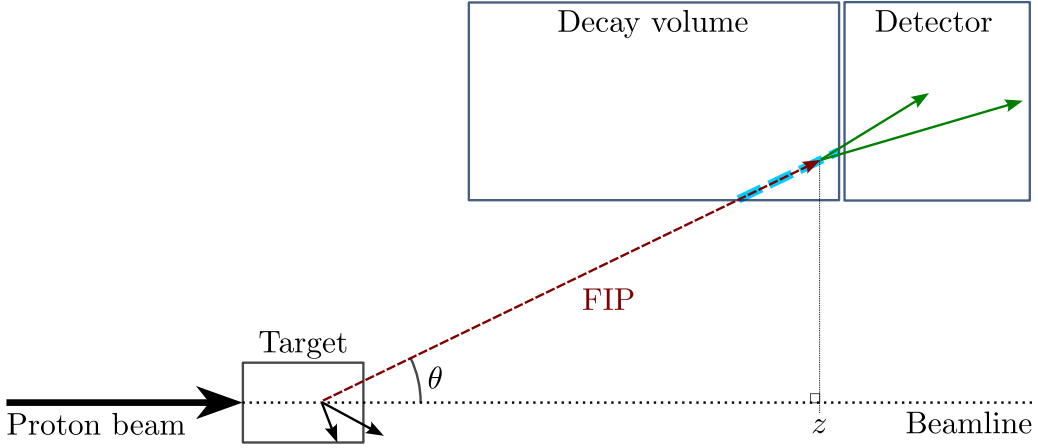

Figure 1. Illustration of the impact of different contributions to the number of events (2.1), taking as an example a beam dump experiment with a detector located downstream of the decay volume. Consider a FIP decaying at coordinates (θ, z), where θ is the polar angle relative to the beamline, z is the longitudinal displacement from the target, and the azimuthal angle ϕ has been omitted from the diagram. The differential probability for a FIP with energy E to decay there is $f(\theta, E)dP_{\text{dec}}/dz$. The azimuthal coordinate ϕ of the decaying FIP (whose trajectory is shown by the red arrow) must be within the decay volume, which restricts the available decay positions to the blue dashed line. These limitations are included in the azimuthal acceptance ϵ_{az}. Next, at least two of the FIP decay products (the green arrows) have to point to the detector; this is accounted for in ϵ_{dec}. Depending on the setup and the FIP, this requirement may significantly limit the decay volume's "useful" angular coverage. In particular, for 2-body decays into stable particles, the decay products can only point to the detector if the decayed FIP also points to the detector. Only the narrow angular domain that the detector covers contributes to the number of events.

The quantities entering Eq. (2.1) are the following (see also Fig. 1):

- $N_{\text{prod}}^{(i)}$ is the total number of FIPs produced by the process i, e.g., decays of mesons, direct production by proton-target collisions, etc. (see fig. 2).

- z, θ and E are, respectively, the position along the beam axis, the polar angle, and the energy of the FIP.

- $f^{(i)}(\theta, E)$ is the differential distribution of FIPs in polar angle and energy, for FIPs produced through the process i.

- $\epsilon_{\text{az}}(\theta, z)$ is the azimuthal acceptance:

$$\epsilon_{\text{az}} = \frac{\Delta\phi_{\text{decay volume}}(\theta, z)}{2\pi} \tag{2.2}$$

where $\Delta\phi$ is the fraction of azimuthal coverage for which FIPs decaying at (z, θ) are inside the decay volume.

- $\frac{dP_{\text{dec}}}{dz}$ is the differential decay probability:

$$\frac{dP_{\text{dec}}}{dz} = \frac{\exp[-r(z, \theta)/l_{\text{dec}}]}{l_{\text{dec}}} \frac{dr(z, \theta)}{dz}, \tag{2.3}$$

with $r = z/\cos(\theta)$ being the modulus of the displacement of the FIP decay position from its production point, and $l_{\text{dec}} = c\tau\sqrt{\gamma^2 - 1}$ is the FIP decay length in the lab frame.

- $\epsilon_{\text{dec}}(m, \theta, E, z)$ is the decay products acceptance, i.e. among those FIPs that are within the azimuthal acceptance, the fraction of FIPs that have at least two decay products that point to the detector and that may be reconstructed. Schematically,

$$\epsilon_{\text{dec}} = \text{Br}_{\text{vis}}(m) \times \epsilon_{\text{dec}}^{(\text{geom})} \times \epsilon_{\text{dec}}^{(\text{other cuts})} \tag{2.4}$$

Here, Br_{vis} denotes the branching ratio of the FIP decays into final states that are detectable; depending on the presence of a calorimeter (EM and/or hadronic), Br_{vis} may encompass only those states featuring at least two charged particles, or it may also include some neutral states such as photons and K_L^0. $\epsilon_{\text{dec}}^{(\text{geom})}$ denotes the fraction of decay products that point to the end of the detector, and $\epsilon_{\text{dec}}^{(\text{other cuts})}$ is the fraction of these decay products that additionally satisfy the remaining cuts (e.g., the energy cut, etc.).

- ϵ_{rec} is the reconstruction efficiency, i.e. among the FIP decays that are within ϵ_{az} and ϵ_{dec}, the fraction of them that the detector can successfully reconstruct.

Most quantities entering Eq. (2.1) can be accurately estimated analytically and cross-checked separately, which makes the approach (2.1) very transparent. Namely, the azimuthal acceptance is completely determined by the geometry of the decay
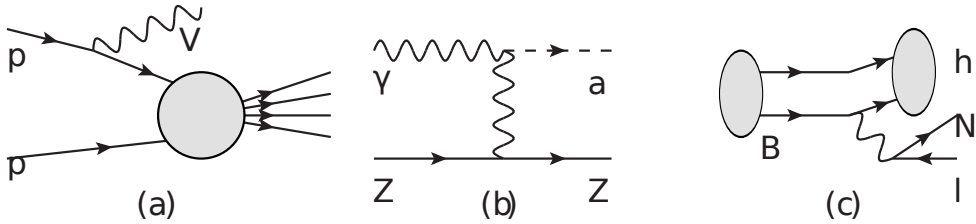
Figure 2. Examples of production processes for various FIPs: (a) proton bremsstrahlung (for the dark photon V), (b) coherent scattering off nuclei (for the ALP a coupling to photons), (c) decays of B mesons into a FIP and another meson h (for HNLs N).

volume, which is typically very simple. Once ϵ_{az} is computed, a simple way to cross-check it is to verify that the integral

$$\mathcal{V} = 2\pi \int d\theta dr r^2(z, \theta) \sin(\theta)\epsilon_{\mathrm{az}} = 2\pi \int d\theta dz \frac{z^2}{\cos^3(\theta)} \sin(\theta)\epsilon_{\mathrm{az}} \qquad (2.5)$$

matches the total volume of the decay volume.

Depending on the production channel, evaluating the FIP distribution function $f^{(i)}(\theta, E)$ may require some external input. This is the case, for instance, for FIPs produced directly in inelastic proton collisions — where one needs to simulate $f^{(i)}(\theta, E)$ using e.g. `PYTHIA 8` to account for showering and hadronization — or for FIPs produced in the interactions of secondary particles, either in their decays or scattering with the material (see Fig. 2 for examples) — where one needs to know the distribution of secondaries $f_{\mathrm{secondary}}(\theta, E)$. Nevertheless, in the latter case, once $f_{\mathrm{secondary}}(\theta, E)$ has been computed, the distribution of FIPs can then be derived analytically without the need for external tools.

ϵ_{dec} may in principle be estimated qualitatively by comparing the opening angle $\Delta\theta_{\mathrm{dec}}$ between the decay products with the angle $\Delta\theta_{\mathrm{det}}$ covered by the detector as seen from the production point. In the simplest case of a 2-body decay into two massless particles, the opening angle is $\Delta\theta_{\mathrm{dec}} \simeq 2\arcsin(\gamma^{-1})$, where γ is the boost factor of the FIP. If $\Delta\theta_{\mathrm{dec}} \gtrsim \Delta\theta_{\mathrm{det}}$, then $\epsilon_{\mathrm{dec}} \approx 0$, otherwise $\epsilon_{\mathrm{dec}} \approx 1$. Because the detector angle is smallest at the beginning of the decay volume while the opening angle decreases as E_{FIP}^{-1}, ϵ_{dec} effectively imposes a cut from below on the FIP energy and the displacement of its decay position from the beginning of the decay volume. If the decay volume is simultaneously the detector (as in the case of, e.g., neutrino detectors), $\epsilon_{\mathrm{dec}}^{(\mathrm{geom})} \equiv 1$.

In order to more accurately estimate ϵ_{dec} — by accounting for the experiment geometry, the presence of a dipole magnet, different FIP decay topologies (such as multi-body decays or decays into unstable particles), and various other selections imposed on the decay products — a *separate* simulation can be performed (see details about the simulation in Sec. 3).

Finally, the computation of ϵ_{rec} would require running the full simulation, including the detector response. As such, it goes beyond the scope of the present semi-analytic approach. However, we believe that it is possible to perform an adequate pre-selection with the help of $\epsilon_{\text{dec}}^{(\text{other cuts})}$ — for instance, by requiring a minimum energy or p_{T} above which the particles are detected with high efficiency (see, e.g., [3]) — such that, conditioned on this pre-selection, $\epsilon_{\text{rec}} \sim \mathcal{O}(1)$.

Last but not least, this semi-analytic method allows for a simple analysis of the number of events in the limit of long lifetimes $c\tau\langle\sqrt{\gamma^2 - 1}\rangle \gg l_{\text{experiment}}$, where $l_{\text{experiment}}$ is the length scale of the experiment. The number of events then reduces to a simple expression:

$$N_{\text{ev}} \approx \sum_i N_{\text{prod}}^{(i)} \cdot \frac{(z_{\text{max}} - z_{\text{min}})}{c\tau} \times \epsilon, \tag{2.6}$$

where ϵ is the total acceptance:

$$\epsilon = \frac{1}{z_{\text{max}} - z_{\text{min}}} \int d\theta dE dz \; \epsilon_{\text{az}} \cdot \frac{\epsilon_{\text{dec}}}{\cos(\theta)\sqrt{\gamma^2 - 1}} \tag{2.7}$$

It may be decomposed as

$$\epsilon = \langle\epsilon_{\text{FIP}}\rangle \times \langle\epsilon_{\text{decay}}\rangle \times \langle(\gamma^2 - 1)^{-1/2}\rangle, \tag{2.8}$$

where $\langle\epsilon_{\text{FIP}}\rangle$ is the mean probability for the FIP to intersect the decay volume, $\langle\epsilon_{\text{decay}}\rangle$ is the mean probability for the decay products to meet the decay products acceptance criteria, and $\langle(\gamma^2 - 1)^{-1/2}\rangle$ is the mean inverse p/m among the FIPs meeting the azimuthal and decay acceptance criteria. This representation is particularly useful when discussing the impact of the geometry on the event rate and when comparing the potential of various experimental setups [27].

The semi-analytic approach presented here is also well suited for estimating the sensitivity to FIP scatterings, which is the main signature in models of light dark matter. In this case, the differential decay probability should be replaced with the scattering probability

$$\frac{dP_{\text{scatt}}}{d\theta dE dz} = n_{\text{detector}} \frac{d^2\sigma_{\text{scatt}}}{d\theta dE}, \tag{2.9}$$

where n_{detector} is the number density of target particles inside the detector, and $d^2\sigma_{\text{scatt}}/d\theta dE$ is the differential cross-section for the scattering of FIPs off the target particles.

2.2 Validation and limitations

The semi-analytic approach presented above has been used to estimate the sensitivities of various experiments at the SPS [22], LHC [16, 23], and FCC-hh [16]. The experimental setups considered cover various options: on-axis and off-axis placements, different decay volume shapes, and different detector orientations relative to
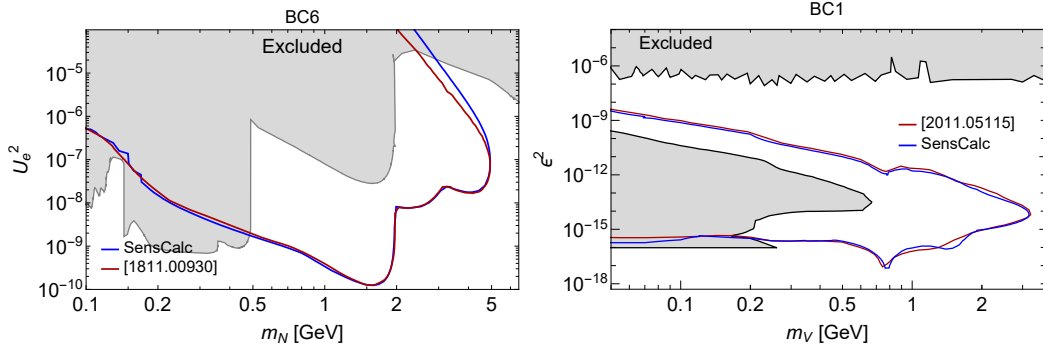
Figure 3. Comparison of the 90% CL sensitivity of the SHiP experiment to heavy neutral leptons (**left panel**) and dark photons (**right panel**), obtained using Eq. (2.1) within the framework of `SensCalc` and derived using the `FairShip` simulations [28, 29]. The old ECN4 configuration of SHiP has been considered here.

the beamline. These estimates, carried out using our semi-analytical method, have been found to be in good agreement with the estimates available in the literature, including simulations-based ones. In particular, Fig. 3 shows the comparison of the sensitivity of the SHiP experiment to heavy neutral leptons (HNLs) and dark photons obtained using Eq. (2.1) with the sensitivity obtained by the SHiP collaboration using the `FairShip` simulation. In the case of dark photons, the slight differences in the sensitivity can be explained by the different elastic proton form factors used to describe the production probability. In the case of HNLs, the discrepancy at the upper bound follows from the monochromatic approximation of the HNL energy spectrum used when computing the sensitivity shown in the SHiP paper [28].

If the assumptions are well-controlled, the semi-analytic approach can agree very well with simulations. Fig. 4 compares the sensitivity of SHADOWS and MATH-USLA to dark scalars as computed via Eq. (2.1) and calculated independently by `SensMC`, a simple weight-based Monte-Carlo that we have implemented as described in Appendix C (see Table 1 for the detailed description of the setup and of the scalar phenomenology used to compute the sensitivity). In these calculations, we did not impose any cuts on the decay products apart from the geometric requirement $\epsilon_{\text{decay}}^{\text{geom}}$; therefore the sensitivities shown are optimistic. The agreement between the two approaches is very good for all masses.

As a further demonstration of the importance of having open-access sensitivity calculations with clear and controllable assumptions and inputs, we have also included in Fig. 4 the sensitivities reported in the respective collaboration papers: the SHADOWS LoI [4], and the MATHUSLA EoI [32]. These sensitivities differ greatly from those we obtained for two main reasons. First, both collaborations use a different description of the scalar production, based on the inclusive estimate where the decay of a B meson into a scalar is described as the decay of its constituent b quark. Second, the assumptions about the experimental setups that have been used

Experiment	SHADOWS	MATHUSLA@CMS
$(x, y, z)_{\min}$, m	(-1,0,14)	(0,60,68)
Fid. dim, m^3	$2.5 \times 2.5 \times 20$	$100 \times 25 \times 100$
Det. dim., m^3	$2.5 \times 2.5 \times 12$	$100 \times 5 \times 100$
Detector plane	xy	xz
Requirement for decay products	Point to the end of detector Oppositely charged, or neutral No other cuts	Point to the end of detector Oppositely charged No other cuts
B distribution	[30]	[17]
Scalar production	Exclusive production, [31]	
Scalar decays	Following [31]	

Table 1. Description of the experimental setups and of the scalar phenomenology used to obtain the sensitivity shown in Fig. 4. The rows indicate respectively: the closest distance from the collision point to the decay volume (the z axis being along the beamline), the decay volume dimensions, the detector dimensions, the orientation of detector layers, the decay products acceptance criteria, the distribution of B mesons used to calculate the flux of scalars, the scalar production branching ratios, and the description of the scalar lifetime and decays. The description of the experiments has been taken from Refs. [4] (SHADOWS) and [32] (MATHUSLA@CMS). For the description of the scalar production, we followed the PBC recommendations [1].

to compute the sensitivity differ from what is actually described in the documents. In the case of SHADOWS, Ref. [4] used not the setup described within that same work (and summarized in Table 1), but a more optimistic setup located closer to the target and the beamline.[3] In the case of MATHUSLA, the acceptance of the decay products was assumed to be 1 in [32]. These differences can significantly affect the reported sensitivity.

Finally, the predictions of our method agree with other publicly available packages — `FORESEE` and `ALPINIST`, as will be discussed in more detail in Sec. 3.2.

The simplicity of our semi-analytic method incurs a number of limitations. First, `SensCalc` cannot provide the full event record associated with each FIP decay or interaction, i.e. the set of all initial, intermediate and final-state particles, including their full kinematics. Instead, it averages over all events that pass the selection. Therefore, it does not allow studying the reconstruction of the FIP parameters, such as its mass, for which the detailed event information is essential. Second, this approach assumes that the surrounding infrastructure does not influence the production of the FIPs. While this is often true in the case of FIPs produced at the collision point or close to it, the situation is different for non-prompt production;

---

[3]From private communications with the representatives of the SHADOWS and MATHUSLA collaborations.
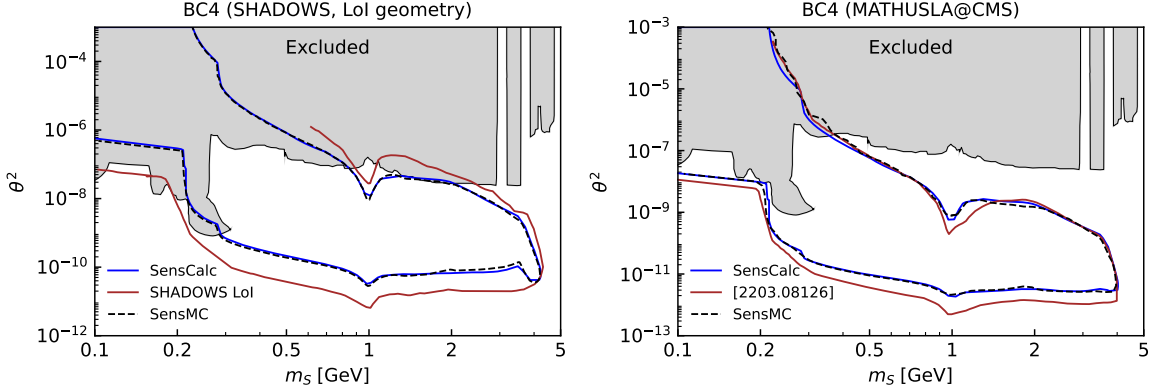
Figure 4. Comparison of the predictions of `SensCalc` (solid blue) with the `SensMC` Monte-Carlo code used for validation (dashed black; described in App. C), for the sensitivity of the experiments located off-axis. SHADOWS (**left**, with the setup described in Ref. [4]) and MATHUSLA [32] (**right**) are considered for the comparison. The description of the experiments has been taken from the collaboration papers. To simplify the comparison and because `SensMC` cannot simulate it, the effect of the dipole magnet has not been included. The numbers of events produced by the two approaches (both with and without including ϵ_{dec}) mostly agree within 20%. Discrepancies are caused mostly by different treatments of the scalar decay and small differences in the numbers describing the production and decay phenomenology of the scalar. The solid red lines show the sensitivities reported in the collaboration documents [4, 32]. The discrepancy between these calculations and our estimates is discussed in the main text.

examples of which include FIPs originating from the decays of long-lived $K^{\pm/0}$ mesons or from neutrino up-scatterings (the neutrino dipole portal [33, 34]), as well as the conversion of photons into axion-like particles (ALPs) in the magnetic field at the LHC [35].

3 SensCalc

3.1 Description

The code `SensCalc` consists of a few `Mathematica` notebooks that compute the number of events for various FIPs (see Table 3 for the list of the currently available models). Four notebooks have to be run sequentially: `Acceptances.nb`, `FIP distribution.nb`, `FIP sensitivity.nb`, and `Plots.nb`, see Fig. 5.

In the first notebook, `Acceptances.nb`, the user specifies the experimental setup — the geometry and dimensions of the decay volume and detector, as well as some details about the detector such as the presence of an ECAL and dipole magnet, see Fig. 6. The list of the experiments currently implemented in `SensCalc` is provided in Table 2. The user can easily implement new experiments, or modify one

Facility	List of experiments
SPS	SHiP [3], NA62$_{\text{dump}}$ [5], HIKE$_{\text{dump}}$ [5], SHADOWS [4]
Fermilab (dump)	DUNE, DUNE-PRISM [36], DarkQuest [8]
LHC	FASER/FASER2/FASERν/FASERν2 [37–39]
	SND@LHC/advSND [12, 39]
	FACET [10], MATHUSLA [32], Codex-b [14], ANUBIS [13]
FCC-hh	Analogs of the LHC-based experiments [16]

Table 2. List of the experiments whose geometry is currently implemented in `SensCalc`, along with, for each experiment, a reference containing a description of the setup used.
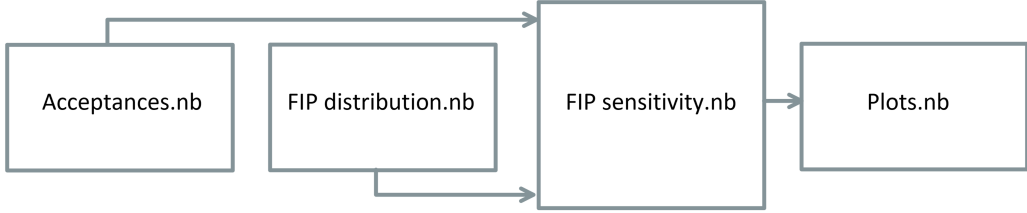

Figure 5. Sketch of the modular structure of `SensCalc`. The notebook `Acceptances.nb` produces the list of acceptances ϵ_{az} and ϵ_{dec} entering Eq. (2.1) for the selected experiment. The notebook `FIP distribution.nb` computes the distribution of FIPs $f(m, \theta, E)$ at the facility housing the experiment. The notebook `FIP sensitivity.nb` uses as input the outputs of the two previous notebooks to calculate the tabulated number of events, and then calculates the sensitivity in the mass-coupling plane as a function of the remaining parameters such as the minimal number of events and any additional model-specific parameters. Finally, `Plots.nb` produces the sensitivity plots from the output of the previous notebook.

of the already implemented setups, which may be useful when optimizing an experiment. Some past experiments are also included: CHARM [40] and BEBC [41] at the SPS. In this notebook, the user must also provide all the relevant quantities such as the number of protons on target (or the integrated luminosity for LHC- and FCC-hh-based experiments), the target material, and the production cross-sections for secondary particles (mesons and heavy bosons). For the implemented experiments, these parameters are already listed in the notebook.

Once the setup is fixed, the notebook evaluates the angular coverage of the experiment and ϵ_{dec} for various FIPs. Concretely, it first defines the grid of the FIP masses m, FIP energies E, and its decay coordinates within the decay volume: the polar angle θ and the longitudinal displacement from the target along the beam axis z. Using these coordinates, the notebook then evaluates $\epsilon_{\text{az}}(\theta, z)$ and the list of azimuthal angles ϕ for which the FIP is inside the decay volume.

Having the grid (E, θ, z, ϕ), the notebook then simulates the FIP decays using its dominant decay channels and calculates the decay acceptance $\epsilon_{\text{dec}}(m, \theta, E, z)$ by
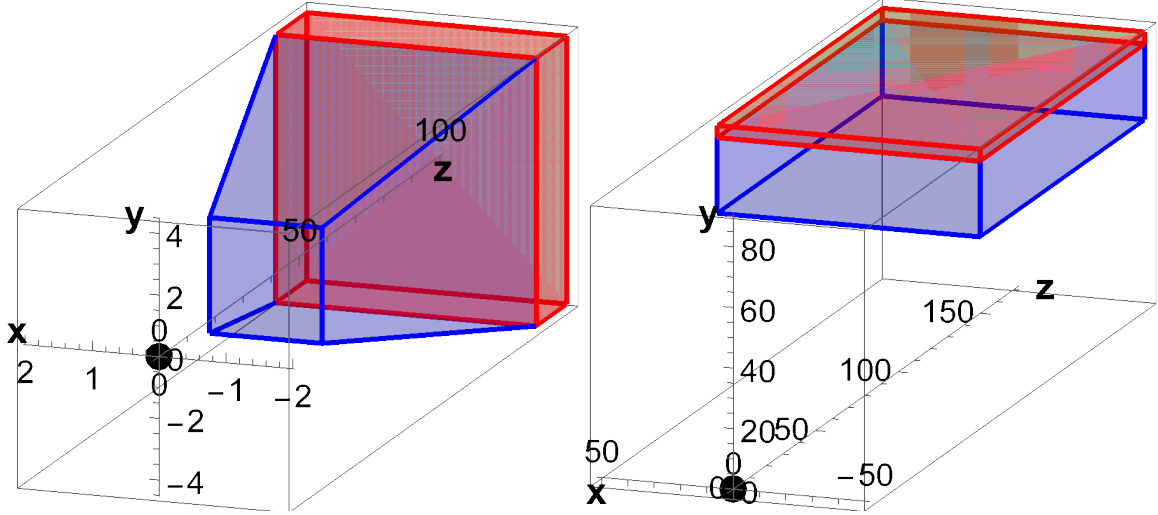
Figure 6. Visualizations of the geometries of the SHiP (**left**) and MATHUSLA (**right**) experiments, as implemented in `SensCalc` (in the notebook `Acceptance.nb`). The blue domain corresponds to the decay volume, while the red domain shows the detector. The descriptions of the two geometries have been taken from the SHiP LoI [3] and Ref. [32].

averaging over these decays and ϕ. The averaging over ϕ is already possible at this stage since the other quantities that determine the number of events (2.1) do not depend on the azimuthal angle. Namely, the differential decay probability dP_{dec}/dz only depends on z and θ, while the FIP distribution function is typically isotropic in ϕ.

The decay channels implemented for each FIP are listed in Table 4. For 3-body decays, the distribution of the decay products is generated taking into account both the phase space and the matrix element of the process. If the FIP decay products are short-lived, the routine decays them until only metastable particles are left. By default, those are $\gamma, e, \mu, K_L^0, \pi^\pm, K^\pm$. The decays of particles with many modes (such as D, B, τ) are approximated by some representative decays; for example, for τ this is a 3-body decay into one charged particle and two neutrinos, while for D, B these are multi-hadronic decays.

Let us now discuss the computation of ϵ_{dec} in more details. The main acceptance criterion is the requirement that the trajectories of at least two decay products with zero total electric charge are within the acceptance of the detector until its final plane. Decays into pure neutral final states (i.e., photons or K_L^0) are also included if a calorimeter is present. If the detector includes a magnetic spectrometer, the components of the charged particles' coordinates and momenta are shifted by a kick right after the magnet in order to approximate the effect of the magnetic field. In addition to this geometric requirement, ϵ_{dec} may also include various kinematic cuts. The implemented cuts include the energy cut, the transverse momentum cut, the transverse impact parameter cut, and the spatial separation cut for neutral particles

in the calorimeter. By complete analogy, the user may impose further kinematic cuts. Although the cuts are applied at the Monte-Carlo truth level, i.e. they are implemented without considering reconstruction effects such as the finite resolution of 4-momenta measurements, they can already give us some understanding of the effects that a realistic event reconstruction would have on the signal yield. Such reconstruction effects could in principle be approximated by e.g. applying some smearing to the kinematics variables of the decay products, according to the detector resolution. Note that the acceptance criterion includes partially reconstructible states, i.e. final states for which the FIP invariant mass cannot be reconstructed from the detected decay products.

The output of the first notebook is a table with the following columns:

$$\{m, \theta, E, z, \epsilon_{\mathrm{az}}, \epsilon_{\mathrm{dec}}\} \tag{3.1}$$

Model	Ref.	Production channels
BC1	[29, 42]	Decays of π, η, η', mixing with ρ^0 Proton bremsstrahlung, Drell-Yan process
BC4, BC5	[31, 43]	2-/3-body decays of B, decay $h \to SS$
BC6-8	[44]	2-/3-body decays of B, D, W
BC9	[18, 45]	Coherent production: Primakov process, pZ scattering Decays of π^0, η
BC10	[1]	B decay
BC11	[18, 46, 47]	Decays of B, mixing with $\pi^0/\eta/\eta'$ Deep-inelastic production

Table 3. FIP production channels in the various models implemented in `SensCalc` with: the benchmark names according to PBC [1], the reference used to describe the production channels, and the list of the production channels implemented in `SensCalc`. The models are dark photons (BC1), dark scalars with Higgs mixing (BC4) and also with the quartic coupling (BC5), Heavy neutral leptons with arbitrary mixing patterns (including the limiting cases of the pure mixing with ν_e, ν_μ, or ν_τ (BC6–BC8)), and ALPs coupling to photons (BC9), fermions (BC10) and gluons (BC11).

The second notebook, `FIP distribution.nb`, computes the angle-energy distribution of the FIPs produced by various facilities and mechanisms. The list of implemented production channels, along with the relevant references used to describe the production, can be found in Table 3. Many production mechanisms require knowing the distributions of the parent particles at the given facility, such as mesons, heavy SM bosons, and photons — including those produced in secondary interactions. We provide them as tabulated distributions in polar angle and energy, which we generate following the literature or just using available distributions from

existing studies (see also Appendix B for a description of how we have generated the distributions of parent particles). Users may easily replace the included distributions with their own differential flux. With the distribution of parent particles at hand, we then derive the distribution of FIPs. If the FIPs are produced in decays, we compute their phase space in the rest frame of the parent particle and then boost it to the lab frame. In the case of 3-body decays, the phase space takes into account the matrix element of the process. For FIPs produced via elastic scattering, we adopt the differential cross-section of the process from existing studies, and then convolve it with the distribution of the parent particles. Should the need arise, new production channels may be added by the user, following the above examples.

Such a derivation of the FIP distribution is not possible, however, in the case of FIPs that are produced inelastically in proton-proton collisions (such as via the Drell-Yan process for dark photons or deep-inelastic production of ALPs through the gluon coupling), which require an external simulation. In this case, we use `MadGraph5_aMC@NLO` (v3.4.2) [48] with a model implemented in `FeynRules` [49] and exported to the UFO format [50]. To account for showering and hadronization, the events simulated in `MadGraph` are further processed by `PYTHIA 8` [51]; see also Appendix B.1 for details. The UFO files and the tabulated FIP distributions are provided alongside `SensCalc`.

The output of the second notebook is a tabulated distribution of the form

$$\{m, \theta, E, f^{(i)}\}, \tag{3.2}$$

where the last column is the value of the FIP distribution function for the given (m, θ, E) and the production mechanism i. Some examples of computed distribution functions are shown in Fig. 7.

Let us highlight an important point. Since the FIP distributions are determined mainly by the kinematics of the collisions, they can be considered identical for the different experiments housed at a same facility, assuming that the colliding particles are the same.[4] For collider experiments, we typically deal with proton-proton collisions, and this notebook only needs to be run once to obtain the distributions. In the case of beam dump experiments, some differences may arise as a result of different target/beam dump compositions. When the FIP is produced via the decays of secondaries, this only affects the overall scaling of the secondaries production cross section, which depends on the atomic number A: $\sigma_{\mathrm{prod,second}} \propto A^{0.29}$ [52]. Therefore, as in the collider case, the notebook only needs to be run once. If, however, the FIP is produced in scattering processes, then different targets may affect not only the normalization but also the shape of the distribution. To take this into account, we generate the fluxes for a few common types of targets.

---

[4]This is not the case for non-prompt production of FIPs, which goes beyond the scope of the present discussion.

Model	Ref.	Decay channels	Decay channels (ϵ_{dec})
BC1	[29, 42]	$ee, \mu\mu, \tau\tau$ $\pi\pi, 3\pi, 4\pi, KK, m \lesssim 2$ GeV $q\bar{q}, m \gtrsim 2$ GeV	$ee, \mu\mu$ $\pi\pi, 4\pi, m_V < 2$ GeV $q\bar{q}, m_V > 2$ GeV
BC4, BC5	[31, 43]	$ee, \mu\mu, \tau\tau,$ $\pi\pi, KK, 4\pi, DD, BB$	$ee, \mu\mu, \tau\tau$ $\pi\pi, KK, DD, \tau\tau, BB$
BC6-8	[44]	$3\nu, ll\nu$ meson $+ l/\nu, m \lesssim 1$ GeV $\nu q\bar{q}, lq\bar{q}', m \gtrsim 1$ GeV	$ll\nu$ $lq\bar{q}'/\nu q\bar{q}, m \geq 1.5$ GeV meson $+ l/\nu, m < 1.5$ GeV
BC9	[18]	$\gamma\gamma$	$\gamma\gamma$
BC10	[1]	$ee, \mu\mu, \tau\tau$	$ee, \mu\mu, \tau\tau$
BC11	[18, 46]	$\gamma\gamma$ $\gamma\pi\pi, \eta\pi\pi, 3\pi, m < 1.5$ GeV $GG, m > 1.5$ GeV	$\gamma\gamma, GG$ $\gamma\pi\pi, \eta\pi\pi$

Table 4. Decay channels of the FIPs implemented in `SensCalc`. From left to right: the model name according to PBC [1] (see also the caption of Table 3), the reference used to describe the decays, the decay channels used to calculate the lifetime τ_{FIP} and the branching ratio of visible decays, and the decay channels used to calculate the decay acceptance ϵ_{dec}.
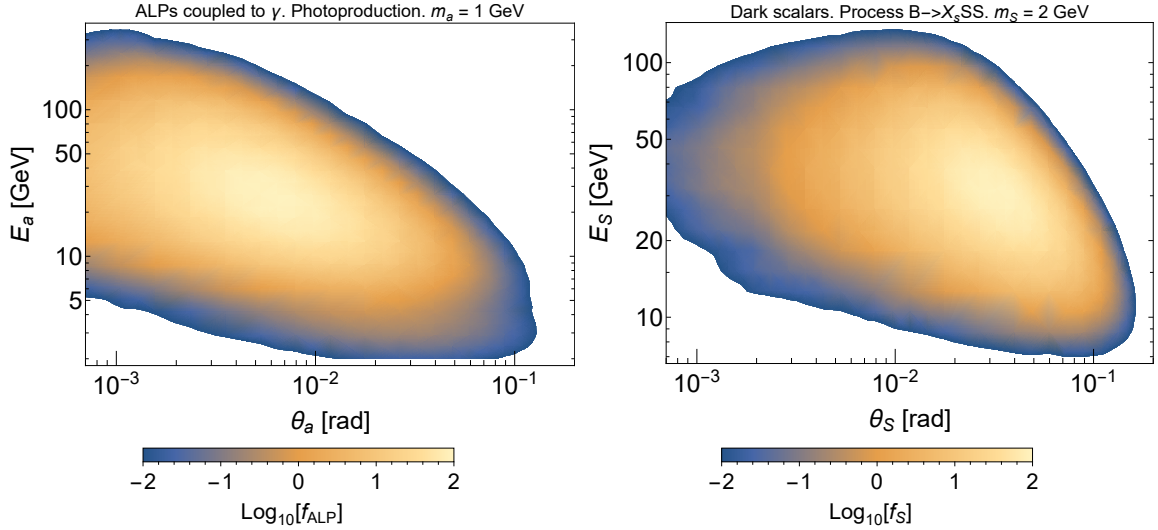

Figure 7. Examples of angle-energy distributions $f^{(i)}(\theta, E)$ for ALPs coupled to photons (**left**) and dark scalars with a non-zero quartic coupling (**right**), produced by the notebook `FIP distribution.nb`.

The notebooks `<FIP> sensitivity.nb` (with `<FIP>` replaced by the actual FIP) evaluate the sensitivity of the chosen experiment to the corresponding FIP. This is done via computing a tabulated number of events. There is a dedicated notebook for each FIP. First, the notebook imports the acceptance data computed by

`Acceptances.nb`, the distributions produced by `FIP distribution.nb`, as well as the relevant quantities defining the FIP phenomenology, such as the production branching ratios, lifetimes, and branching ratios of the decays into visible states at the given experiment. It then maps them to logarithmic scale and interpolates them to obtain the functions entering Eq. (2.1).

Depending on the FIP, there may exist uncertainties in the description of its production and decay, which may significantly affect the event rate. This is the case, e.g., for dark scalars, where one may describe their production inclusively or exclusively; and for dark photons, for which the description of the proton bremsstrahlung channel depends on the maximal allowed p_T and on the minimal energy allowed to be transferred to the dark photon. The user has the freedom to tune these parameters.

In addition, there may exist model-specific parameters that must be selected before performing the computation. For instance, in the case of HNLs, this is their nature (Dirac or Majorana) and their mixing pattern $U_e^2 : U_\mu^2 : U_\tau^2$.
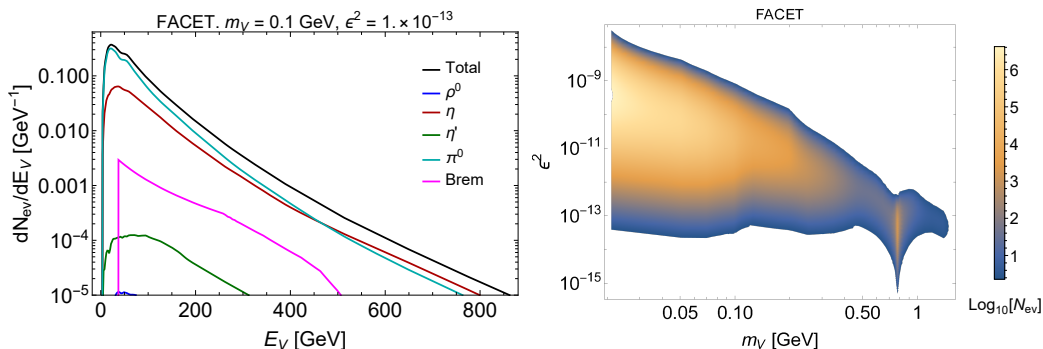

Figure 8. Examples of the output produced by the notebook `FIP sensitivity.nb`. **Left panel**: differential number of events with respect to the FIP's energy for various production channels. **Right panel**: density plot of the total number of events as a function of the FIP mass and coupling. As an example, dark photons at FACET are considered. No cuts on the decay products other than the geometric acceptance have been applied.

During the computation, this notebook produces intermediate results that may be useful for the sensitivity analysis. This includes the differential number of events with respect to θ, E, or z, as well as the number of events as a function of the mass and coupling, see Fig. 8. Last but not least, the notebook also shows the behavior of the overall acceptances ϵ, cf. Eq. (2.7).

Once the tabulated number of events has been produced, the notebook computes the sensitivities. To this end, the user needs to select the critical number of events as well as some model-specific parameters. For example, for dark scalars, one needs to specify the value of the branching ratio $\mathrm{Br}(h \to SS)$, which is non-zero in the presence of the quartic coupling $\mathcal{L} \propto hSS$ (see Appendix A for detail). Because the critical number of events can be freely specified, the user can compute both "exclusion" sensitivity limits — corresponding to 2.3 expected events at 90% CL — or

"discovery" sensitivity limits by (externally) providing the critical N_{ev} corresponding to the desired significance level and background expectation.

Finally, the notebook `Plots.nb` plots the sensitivities obtained in the previous notebook. It scans over available sensitivity files, imports those needed by the user, and finally produces the figures (see e.g. Fig. 9).
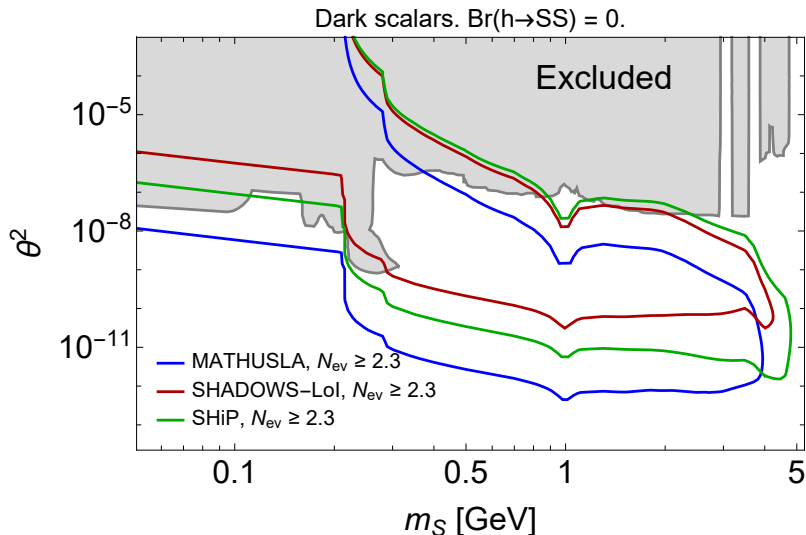

Figure 9. Example of a sensitivity plot produced by the notebook `Plots.nb`, for the model of dark scalars.

The user interaction with the various notebooks, such as choosing the experiment, selecting the cuts and the particular FIP model, is organized via dialog windows. This makes running the notebooks straightforward for FIPs and experiments that are already implemented.

To successfully run the notebooks, the user needs to install two dependencies: `FeynCalc` [53], which is a `Mathematica` package for the symbolic evaluation of Feynman diagrams, and a `C` compiler that is recognized by `Mathematica`.

The performance of the code has been tested on various machines and operating systems. For instance, on a Windows laptop with 16 GB of RAM, 8 CPU cores, and `Mathematica 12.1`, the typical time required to compute the sensitivity from scratch is $\mathcal{O}(1\ \text{hour})$ — depending on the FIP type and on the mass-coupling grid density. This time is reduced if the FIP distribution has already been pre-generated.

`SensCalc` still offers significant potential for further improvement. Of particular interest would be the possibility to compute the sensitivity to additional FIP models, including those for which the main signature is scatterings with the detector material. Another well-motivated extension would be to support ALPs with an arbitrary coupling pattern.

A particularly interesting improvement would be to implement an approximate description of the hadronic decays of heavy FIPs ($m_{\rm FIP} \gg 1$ GeV). Currently, `SensCalc` describes them perturbatively – via decays into quarks and gluons. Their subsequent showering and hadronization in-flight would require external tools such as `PYTHIA 8`, and hence goes beyond the scope of the present semi-analytic approach.[5] However, it may be possible to implement this feature approximately, for instance by simulating the phase space of FIP decays for several masses in `PYTHIA 8`, then selecting typical sets of decay products, and finally using their pre-computed phase space when evaluating the decay products acceptance.

Finally, the implementations of the various experiments should be updated according to their latest specifications, which may differ from those listed in currently available documents. This may be done by contacting the representatives of the collaborations.

We are planning to add the above features in a future code update.

3.2 Comparison with similar software packages

At the moment of releasing `SensCalc`, there are two publicly available codes for computing the sensitivity of lifetime-frontier experiments to decaying FIPs: `FORESEE` [17] and `ALPINIST` [18].

`FORESEE` is a `Python`-based code developed to evaluate the sensitivities of the far-forward experiments at the LHC and FCC-hh. The currently implemented models of FIPs include dark scalars, dark photons, ALPs coupling to W bosons, millicharged particles, and up-philic scalars. The package includes the tabulated distributions of various SM particles, including photons, mesons, and heavy bosons. Apart from the tabulated number of events as a function of the FIP mass and coupling, it can additionally produce detailed event records in the `HepMC` format, which may then be passed to e.g. a detector simulation software. By default, `FORESEE` does not calculate the acceptance of the decay products; instead it only requires the FIP to decay inside the decay volume, although the user may impose various cuts.

`ALPINIST` computes the sensitivity of extracted-beam experiments — including those at the SPS, Fermilab, and some past experiments — to ALPs couplings to various SM particles. Its modules use `Mathematica, ROOT`, and `Python`. The prominent feature of the code is that it can handle generic ALPs with simultaneous couplings to W bosons, gluons, and the $U_Y(1)$ field. Unlike `FORESEE`, the computation also incorporates the reconstruction of the decay products inside a detector, at the price

---

[5]Nevertheless, the accuracy of the current method remains surprisingly good even in this regime. This can be understood as follows: because the momentum flow of the hadronized decay products is determined by the kinematics of the incoming jets, the geometric part of $\epsilon_{\rm dec}$ (Eq. (2.4)) still describes the decay adequately. This qualitative argument is in agreement with Fig. 3: the dominant decays of the HNLs and dark photons with mass $m_{\rm FIP} \gtrsim 1$ GeV include a quark-antiquark pair, and nevertheless, the semi-analytic approach agrees well with simulations.
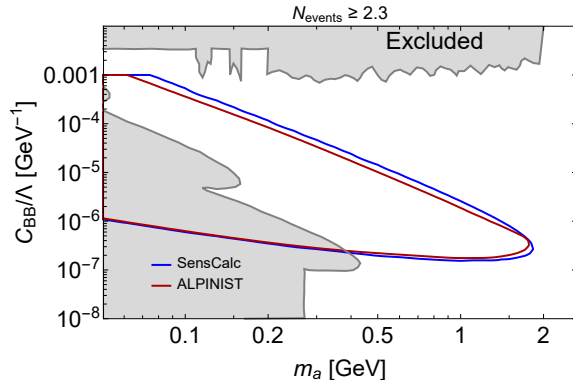
Figure 10. Comparison of the sensitivity of SHiP to ALPs coupling to photons as computed by `SencCalc` (blue line) and `ALPINIST` [18] (red line). The definition of the coupling, as well as the fractions of mesons leading to the production of ALPs via photo-conversion, are taken from Ref. [18]. The use of different setups for SHiP in the sensitivity calculations may explain the discrepancy at the upper bound: we have used the currently considered ECN3 configuration from Ref. [3], for which the decay volume is located 12 m closer to the target, while Ref. [18] considers the old configuration from Ref. [54].

of a longer computation time to obtain the tabulated number of events. Only fully reconstructible states are considered. The output of `ALPINIST` consists of data files with the mass-coupling dependence of the number of events for various production and decay modes.

The predictions of `SensCalc` agree well with the results of `ALPINIST` (see Fig. 10) and FORESEE (the comparison between the semi-analytic approach and FORESEE is discussed in Ref. [23]).

Unlike these two software packages, `SensCalc` is not restricted to a particular facility. In addition, among the implemented FIP models, it considers for the first time HNLs with arbitrary mixing patterns. The main limitation of `SensCalc` compared to `FORESEE` is that it cannot generate detailed event records, while compared to `ALPINIST`, it is that it does not (currently) consider generic ALPs and does not perform a detailed event reconstruction.

4 Conclusion

Feebly interacting particles (FIPs) are present in a broad class of new-physics scenarios that attempt to resolve the known problems of the Standard Model. Their search at various facilities and experiments collectively forms the lifetime frontier of particle physics. During the last decade, many lifetime-frontier experiments have been proposed, that differ in the housing facility, geometric location, and detector technology. With a few exceptions, most of these experiments are not approved yet, and their design is not finalized. Their sensitivities to FIPs are computed by the col-

laboratories themselves, using internal tools which are not publicly accessible. This makes it difficult to control the inputs to the computations, such as the model of the production and decay. It is therefore crucial to have a publicly available tool for computing the sensitivity of those experiments to various FIPs in a uniform, fast and well-controlled way.

The present paper addresses this issue by presenting `SensCalc` — a `Mathematica`-based code for evaluating the sensitivity of various experiments to decaying, long-lived FIPs, based on a semi-analytic approach developed in a number of previous studies (see Sec. 2.1) and cross-checked against various state-of-the-art packages (see Sec. 2.2).

`SensCalc` already supports a broad range of models and experiments (see Sec. 3.1), with more to be added in future versions. Models currently implemented include dark photons, dark scalars, heavy neutral leptons with various mixing patterns, and axion-like particles coupled to different SM particles. Numerous experiments have been implemented, located at any of the following facilities: the SPS, LBNE, LHC, and FCC-hh. The user retains full control over every aspect of the sensitivity calculation: from the geometry of the experiment and the distribution of the FIP's parent particles to the branching ratios of the FIP production/decay modes and the requirements on the decay products. Besides contributing to the transparency and trustworthiness of the results, this also allows users to easily modify the underlying assumptions as needed, or to add their own models and experiments to `SensCalc`.

By publicly providing a transparent, semi-analytic method to consistently compute the expected signal at various lifetime-frontier experiments, `SensCalc` can help address the discrepancies that currently exist in the literature between the descriptions of FIPs and acceptances employed by different collaborations. This is a timely and necessary contribution to the field of FIP searches, as many experiments are currently undergoing active development and optimization, while funding bodies and hosting facilities must decide which projects to prioritize. `SensCalc` can help with the former by providing fast (re-)calculation of the expected signal as the experiment's design evolves, and with the latter by ensuring a fair and consistent comparison of the expected signals between the proposed experiments, with well-controlled assumptions thanks to a uniform and well-validated implementation of the official PBC benchmarks. This could be particularly relevant in the context of the ECN3 hall upgrade at the CERN SPS, in which a number of experiments are currently being considered for inclusion, namely HIKE, SHiP, and SHADOWS.

Conflict of Interest Statement

The authors of the present manuscript are also members of the SHiP collaboration, which represents one of the experimental proposals currently competing for funding and access to facilities, notably as part of the ongoing Physics Beyond Colliders study and in the context of the upcoming upgrade of the ECN3 hall at CERN. The present manuscript solely reflects the authors' views, and not those of the SHiP collaboration.

A   Uncertainties in the description of FIPs

A.1   Discrepancies in the literature

The description of the FIP production and decay, and sometimes even the definition of the FIP couplings, may vary among the sensitivity estimates performed by the different collaborations. One example is the dark scalar S. Following the PBC report [1], the SHiP collaboration uses the exclusive description of the production of S, while other collaborations adopt instead the inclusive description (see the discussion in Ref. [55]). In the domain $m_S \gtrsim 2 - 3$ GeV, where the inclusive approach breaks down, the difference in the number of produced scalars between these two descriptions may be a factor of 20 or more. Another problem arises from the theoretical uncertainty on the hadronic decay width, which may be as large as a factor of 100 [43, 55] (see also a recent discussion in Ref. [56]). While SHiP and SHADOWS assume the decay width computed in Ref. [43], the FASER collaboration [57] uses the decay width from Ref. [58]. Depending on the calculation used, the sensitivity may therefore differ significantly.

Another example is with ALPs a coupling to gluons. The PBC report defines an interaction of the form $\mathcal{L} \propto a g_a G^{\mu\nu,a} \tilde{G}^a_{\mu\nu}$, where $G^{\mu\nu}$ is the gluon field strength and g_a is a fixed dimensionful coupling. Theoretical works often [46, 47] adopt a different definition, $\mathcal{L} \propto a g_s^2 g_a G^{\mu\nu,a} \tilde{G}^a_{\mu\nu}$, where $g_s = g_s(m_a)$ is the QCD coupling. The latter definition is used by `ALPINIST` [18] for computing the sensitivity of beam dump experiments to ALPs (and their results are used by the SHiP, HIKE, and SHADOWS collaborations in Ref. [59]). Furthermore, while some collaborations [14] include the production of ALPs through gluon fusion, others do not (this is the case in particular of `ALPINIST` [18]).

Another problem arises with ALPs that couple to fermions. The PBC [1] recommends including only the decays into leptons in the total width — even though it may be dominated by hadronic decays in the mass range $m_a \gtrsim 2m_\pi$ — while some collaborations also include hadronic channels [14].

Such mismatches between the assumptions used to compute different sensitivities are particularly problematic when said sensitivities are shown in the same plot — such as e.g. in the FIPs 2022 proceedings [59] — without emphasizing that the underlying assumptions differ.

A.2 Definition of the FIP couplings used in `SensCalc`

The effective Lagrangians of the models implemented in `SensCalc` are:

– **BC1** (dark photons):

$$\mathcal{L}_{\text{int}} = -\epsilon e V_\mu J^\mu_{\text{EM}} \tag{A.1}$$

where V_μ is the dark photon field, J^μ_{EM} is the EM current, and $e = \sqrt{4\pi\alpha_{\text{EM}}}$ is the EM coupling.

– **BC4** and **BC5** (dark scalars):

$$\mathcal{L}_{\text{eff}} \supset m_h^2 \theta h S + \frac{\alpha}{2} h S^2, \tag{A.2}$$

where θ is the mixing angle and α is the quartic coupling. By default, the sensitivity is evaluated assuming a constant branching ratio $\text{Br}(h \to SS) \propto \alpha^2$.

– **BC6, BC7, BC8** (HNLs):

$$\mathcal{L}_{\text{int}} = \sum_{\alpha=e,\mu,\tau} U_\alpha \bar{N} \left(\frac{g}{\sqrt{2}} \gamma^\mu P_L l_\alpha W_\mu + \frac{g}{2\cos(\theta_W)} \gamma^\mu P_L \nu_\alpha Z_\mu \right) + \text{h.c.}, \tag{A.3}$$

where N is the HNL, U_α the mixing angle, g the weak coupling, and $l_\alpha, \nu_\alpha, W, Z$ the SM fields. The HNL may be either a Dirac or a Majorana particle.

– **BC9** (ALPs coupling to photons):

$$\mathcal{L}_{\text{int}} = \frac{g_a}{4} a F_{\mu\nu} \tilde{F}^{\mu\nu}, \tag{A.4}$$

where a is the ALP field, g_a is a dimensionful coupling, and $F_{\mu\nu}$, $\tilde{F}_{\mu\nu} = \frac{1}{2}\epsilon_{\mu\nu\alpha\beta}F^{\alpha\beta}$ are the EM field strength and its dual.

– **BC10** (ALPs coupling to fermions):

$$\mathcal{L}_{\text{int}} = \frac{g_Y}{2v_H}(\partial_\mu a)\sum_\alpha \bar{f}\gamma^\mu\gamma_5 f, \tag{A.5}$$

where g_Y is a dimensionless coupling, $v_H \approx 246$ GeV is the Higgs VEV, and f are SM fermions.

– **BC11** (ALPs coupling to gluons):

$$\mathcal{L}_{\text{int}} = g_a g_s^2 a G_{\mu\nu}^a \tilde{G}^{\mu\nu,a}, \tag{A.6}$$

where g_s is the strong coupling constant, a is the ALP field, g_a is a dimensionful constant, $G_{\mu\nu}^a$ is the gluon field strength, and $\tilde{G}_{\mu\nu}^a = \frac{1}{2}\epsilon_{\mu\nu\alpha\beta}G^{\alpha\beta,a}$ is its dual field strength. Everywhere except for the production of ALPs from DIS, we follow the definition of g_s from Ref. [18]. In the DIS case, we employ the running of g_s associated with the default PDF set in `MadGraph`.

B Inputs used for generating the FIP distributions

B.1 DIS processes

DIS production channels are relevant for several FIPs considered in `SensCalc`: dark photons and ALPs with the gluon coupling. We simulate the production of these particles in `MadGraph5_aMC@NLO`, interfaced with `PYTHIA 8` for showering and hadronization. The hard processes that we simulate are the lowest-order and next-to-lowest-order processes for quark and gluon fusion:

$$q + \bar{q} \to V, \quad q + \bar{q} \to V + j, \quad G + G \to a, \quad G + G \to a + j \tag{B.1}$$

As for the scale of the process, we choose the invariant mass of the quark-antiquark pair (`dynamical_scale_choice = 4`). Although `SensCalc` already includes the tabulated angle-energy distributions of the FIPs produced by DIS, it also includes the UFO files for the models of dark photons and ALPs, allowing the user to re-generate the distributions under different assumptions if needed.

The DIS production suffers from significant theoretical uncertainties. First, the choice of scale becomes important for light FIPs with masses $m_{\text{FIP}} \simeq 1 - 2$ GeV, where the uncertainties in the production cross-section may become $\mathcal{O}(1)$. Second, the minimal parton energy fraction required to produce a FIP is $x_{\text{min}} = m_{\text{FIP}}^2/s_{\text{pp}}$. For experiments like the LHC/FCC-hh and GeV-scale FIPs, x_{min} can be as tiny as 10^{-8}; this domain is only explored experimentally and is therefore subject to theoretical uncertainties (see Ref. [61]). This becomes especially problematic in the case of the FCC-hh. Because of this, we do not consider the DIS production channel for the FCC-hh-based experiments.

Particle	LBNE	SPS	LHC	FCC-hh
$\pi^0/\eta/\eta'/\gamma$	[45]	[45]	[60]	[60]
B, D	[18]	[30]	[17]	[17]
W, h, Z	–	–	[17]	[17]

Table 5. List of the references used to generate, or directly take, the distributions of secondary particles that may produce FIPs.

B.2 Production by secondary particles

Another important FIP production mechanism is through secondary particles — either in their decays or scatterings. We handle this case by either generating the distributions of secondary particles using approaches from the literature, or directly using pre-calculated distributions. The list of references is provided in Table 5.

C `SensMC`: a simplified Monte-Carlo used for validation

As an additional cross-check of `SensCalc`, we have implemented `SensMC` [26], a small, customizable weight-based Monte-Carlo simulation, as an alternative way of numerically integrating Eq. (2.1) for FIPs produced in meson decays. It makes extensive use of importance sampling in order to handle the (typically tiny) branching ratios of mesons to FIPs and the (possibly very displaced) decay vertex of the FIP. `SensMC` is written in the `Julia` programming language [62] in order to combine performance and readability, and it is released alongside `SensCalc` in the same repository [20], as well as on GitHub.[6]

    `SensMC` numerically estimates Eq. (2.1) using Monte-Carlo integration with importance sampling, by randomly generating a large number of weighted samples whose expectation values are N_{ev}, and finally averaging them. The value of each random sample is computed as follows:

1. A meson species is randomly sampled based on the proportion of produced mesons of this species, with the event weight initially set to the total number of mesons produced across all species. The meson momentum is then randomly sampled from a precomputed spectrum (either a list for the spectrums from `FairShip` [28] or a grid for those from `FORESEE` [17]). To account for potential variations in the atomic weight of the target, that would affect the overall normalization of the spectrums, the event is optionally reweighted using the formula $w_A = w_{\mathrm{Mo}}(A/96)^{0.29}$ [52], with A denoting the atomic weight of the target and assuming that the spectrums were initially computed for a molybdenum target (as is the case for the `FairShip` spectrums).

---

[6]The GitHub repository can be found at `https://github.com/JLTastet/SensMC`.

2. The FIP production channel is randomly selected with a probability proportional to its branching ratio, and the event is reweighted by the total branching ratio to FIPs of the particular meson species. Upon the decay of the parent meson, the momenta of its decay products, including the FIP, are uniformly sampled in phase space. The present simulation currently does not take into account the matrix elements because it cannot compute them all, however the logic needed to handle them is already present, allowing the user to implement their own matrix elements if needed.

3. The FIP's decay vertex is then selected randomly along its trajectory by either a) sampling the proper lifetime from an exponential distribution and calculating the corresponding distance in the lab frame or b) employing importance sampling, which restricts the position of the decay vertex to a shell covering the full decay volume, and then reweights the event by the ratio of the true decay distribution to the importance distribution. The FIP decay mode is selected similarly to its production mode, with a sampling probability proportional (and in most cases equal) to its branching ratio; and the event is reweighted by the total branching ratio of the implemented channels. The momenta of the FIP decay products are uniformly sampled in phase space in the current version (but matrix elements could in principle be taken into account, just like for the FIP production).

4. Following a similar procedure, any unstable Standard Model particles are recursively decayed until only metastable particles (that live long enough to be detected) remain, assuming the branching ratios listed in the `particletools` Python package. The acceptance condition is then evaluated on the set of final metastable particles produced in the FIP decay. The event weight is recorded, along with whether the event is accepted or not.

Because each event is initially weighted by the total number of mesons, all event weights must finally be divided by the number of generated events. The sum of weights then provides a numerical estimate of the total number of physical events (with the FIP decay within the "shell" in case importance sampling is used), while the sum of event weights multiplied by their corresponding (binary) acceptances gives the total number of accepted events, and is independent of the specific importance distribution as long as it fully covers the decay volume.

The sensitivity curve is computed iteratively, starting from a coarse grid in $(\log(m), \log(\theta))$ that covers the region where the experiment is susceptible to be sensitive. The expected number of accepted events is computed at each grid point. The multi-dimensional bisection method (MDBM) [63] is then used to iteratively refine the grid in the vicinity of the iso-contour corresponding to (for example) 2.3 accepted events (for an exclusion sensitivity at the 90% confidence level), effectively

bisecting it without the need to evaluate a dense grid, which would be computationally costly. The final curve is then obtained from bilinear interpolation of the sparse grid values.

References

[1] J. Beacham et al., *Physics Beyond Colliders at CERN: Beyond the Standard Model Working Group Report*, *J. Phys. G* **47** (2020), no. 1 010501, [`arXiv:1901.09966`].

[2] S. Alekhin et al., *A facility to Search for Hidden Particles at the CERN SPS: the SHiP physics case*, *Rept. Prog. Phys.* **79** (2016), no. 12 124201, [`arXiv:1504.04855`].

[3] **SHiP** Collaboration, O. Aberle et al., *BDF/SHiP at the ECN3 high-intensity beam facility*, tech. rep., CERN, Geneva, 2022.

[4] **SHADOWS** Collaboration, M. Alviggi et al., *SHADOWS Letter of Intent*, tech. rep., CERN, Geneva, 2022.

[5] **HIKE** Collaboration, E. Cortina Gil et al., *HIKE, High Intensity Kaon Experiments at the CERN SPS: Letter of Intent*, tech. rep., CERN, Geneva, 2022. Letter of Intent submitted to CERN SPSC. Address all correspondence to hike-eb@cern.ch.

[6] **DUNE** Collaboration, B. Abi et al., *Deep Underground Neutrino Experiment (DUNE), Far Detector Technical Design Report, Volume II: DUNE Physics*, `arXiv:2002.03005`.

[7] **DUNE** Collaboration, B. Abi et al., *Prospects for beyond the Standard Model physics searches at the Deep Underground Neutrino Experiment*, *Eur. Phys. J. C* **81** (2021), no. 4 322, [`arXiv:2008.12769`].

[8] B. Batell, J. A. Evans, S. Gori, and M. Rai, *Dark Scalars and Heavy Neutral Leptons at DarkQuest*, *JHEP* **05** (2021) 049, [`arXiv:2008.08108`].

[9] **MATHUSLA** Collaboration, H. Lubatti et al., *Explore the lifetime frontier with MATHUSLA*, *JINST* **15** (2020), no. 06 C06026, [`arXiv:1901.04040`].

[10] S. Cerci et al., *FACET: A new long-lived particle detector in the very forward region of the CMS experiment*, *JHEP* **2022** (2022), no. 06 110, [`arXiv:2201.00019`].

[11] **FASER** Collaboration, A. Ariga et al., *Technical Proposal for FASER: ForwArd Search ExpeRiment at the LHC*, `arXiv:1812.09139`.

[12] **SHiP** Collaboration, C. Ahdida et al., *SND@LHC*, `arXiv:2002.08722`.

[13] M. Bauer, O. Brandt, L. Lee, and C. Ohm, *ANUBIS: Proposal to search for long-lived neutral particles in CERN service shafts*, `arXiv:1909.13022`.

[14] G. Aielli et al., *Expression of interest for the CODEX-b detector*, *Eur. Phys. J. C* **80** (2020), no. 12 1177, [`arXiv:1911.00481`].

[15] D. Dercks, H. K. Dreiner, M. Hirsch, and Z. S. Wang, *Long-Lived Fermions at AL3X*, *Phys. Rev. D* **99** (2019), no. 5 055020, [`arXiv:1811.01995`].

[16] A. Boyarsky, O. Mikulenko, M. Ovchynnikov, and L. Shchutska, *Exploring the potential of FCC-hh to search for particles from B mesons*, *JHEP* **01** (2023) 042, [`arXiv:2204.01622`].

[17] F. Kling and S. Trojanowski, *Forward experiment sensitivity estimator for the LHC and future hadron colliders*, *Phys. Rev. D* **104** (2021), no. 3 035012, [arXiv:2105.07077].

[18] J. Jerhot, B. Döbrich, F. Ertas, F. Kahlhoefer, and T. Spadaro, *ALPINIST: Axion-Like Particles In Numerous Interactions Simulated and Tabulated*, *JHEP* **07** (2022) 094, [arXiv:2201.05170].

[19] Wolfram Research, Inc., "Mathematica, Version 13.2." Champaign, IL, 2022.

[20] M. Ovchynnikov, *SensCalc, https://doi.org/10.5281/zenodo.7957785*, 2023.

[21] K. Bondarenko, A. Boyarsky, M. Ovchynnikov, and O. Ruchayskiy, *Sensitivity of the intensity frontier experiments for neutrino and scalar portals: analytic estimates*, *JHEP* **08** (2019) 061, [arXiv:1902.06240].

[22] I. Boiarska, A. Boyarsky, O. Mikulenko, and M. Ovchynnikov, *Constraints from the CHARM experiment on heavy neutral leptons with tau mixing*, *Phys. Rev. D* **104** (2021), no. 9 095019, [arXiv:2107.14685].

[23] M. Ovchynnikov, V. Kryshtal, and K. Bondarenko, *Sensitivity of the FACET experiment to Heavy Neutral Leptons and Dark Scalars*, *JHEP* **02** (2023) 056, [arXiv:2209.14870].

[24] P. Coloma, J. López-Pavón, L. Molina-Bueno, and S. Urrea, *New Physics searches using ProtoDUNE and the CERN SPS accelerator*, arXiv:2304.06765.

[25] B. Batell, W. Huang, and K. J. Kelly, *Keeping it Simple: Simplified Frameworks for Long-Lived Particles at Neutrino Facilities*, arXiv:2304.11189.

[26] J.-L. Tastet, *SensMC, https://github.com/JLTastet/SensMC*, 2023.

[27] K. Bondarenko, A. Boyarsky, O. Mikulenko, R. Jacobsson, and M. Ovchynnikov, *Towards the optimal beam dump experiment to search for feebly interacting particles*, arXiv:2304.02511.

[28] **SHiP** Collaboration, C. Ahdida et al., *Sensitivity of the SHiP experiment to Heavy Neutral Leptons*, *JHEP* **04** (2019) 077, [arXiv:1811.00930].

[29] **SHiP** Collaboration, C. Ahdida et al., *Sensitivity of the SHiP experiment to dark photons decaying to a pair of charged particles*, *Eur. Phys. J. C* **81** (2021), no. 5 451, [arXiv:2011.05115].

[30] **SHiP** Collaboration, H. Dijkstra and T. Ruf, *Heavy Flavour Cascade Production in a Beam Dump*, Dec, 2015. CERN-SHiP-NOTE-2015-009.

[31] I. Boiarska, K. Bondarenko, A. Boyarsky, V. Gorkavenko, M. Ovchynnikov, and A. Sokolenko, *Phenomenology of GeV-scale scalar portal*, *JHEP* **11** (2019) 162, [arXiv:1904.10447].

[32] **MATHUSLA** Collaboration, C. Alpigiani et al., *Recent Progress and Next Steps for the MATHUSLA LLP Detector*, in *2022 Snowmass Summer Study*, 3, 2022. arXiv:2203.08126.

[33] M. Ovchynnikov, T. Schwetz, and J.-Y. Zhu, *Dipole portal and neutrinophilic scalars at DUNE revisited: The importance of the high-energy neutrino tail*, *Phys. Rev. D* **107** (2023), no. 5 055029, [`arXiv:2210.13141`].

[34] P. Ballett, T. Boschi, and S. Pascoli, *Heavy Neutral Leptons from low-scale seesaws at the DUNE Near Detector*, *JHEP* **03** (2020) 111, [`arXiv:1905.00284`].

[35] F. Kling and P. Quílez, *ALP searches at the LHC: FASER as a light-shining-through-walls experiment*, *Phys. Rev. D* **106** (2022), no. 5 055036, [`arXiv:2204.03599`].

[36] **DUNE** Collaboration, V. Hewes et al., *Deep Underground Neutrino Experiment (DUNE) Near Detector Conceptual Design Report*, *Instruments* **5** (2021), no. 4 31, [`arXiv:2103.13910`].

[37] **FASER** Collaboration, A. Ariga et al., *FASER: ForwArd Search ExpeRiment at the LHC*, `arXiv:1901.04468`.

[38] **FASER** Collaboration, H. Abreu et al., *Technical Proposal: FASERnu*, `arXiv:2001.03073`.

[39] J. L. Feng et al., *The Forward Physics Facility at the High-Luminosity LHC*, *J. Phys. G* **50** (2023), no. 3 030501, [`arXiv:2203.05090`].

[40] **CHARM** Collaboration, F. Bergsma et al., *A Search for Decays of Heavy Neutrinos*, *Phys. Lett. B* **128** (1983) 361.

[41] **BEBC WA66** Collaboration, H. Grassler et al., *Prompt Neutrino Production in 400-GeV Proton Copper Interactions*, *Nucl. Phys. B* **273** (1986) 253–274.

[42] P. Ilten, Y. Soreq, M. Williams, and W. Xue, *Serendipity in dark photon searches*, *JHEP* **06** (2018) 004, [`arXiv:1801.04847`].

[43] M. W. Winkler, *Decay and detection of a light scalar boson mixing with the Higgs boson*, *Phys. Rev. D* **99** (2019), no. 1 015018, [`arXiv:1809.01876`].

[44] K. Bondarenko, A. Boyarsky, D. Gorbunov, and O. Ruchayskiy, *Phenomenology of GeV-scale Heavy Neutral Leptons*, *JHEP* **11** (2018) 032, [`arXiv:1805.08567`].

[45] B. Döbrich, J. Jaeckel, and T. Spadaro, *Light in the beam dump - ALP production from decay photons in proton beam-dumps*, *JHEP* **05** (2019) 213, [`arXiv:1904.02091`]. [Erratum: JHEP 10, 046 (2020)].

[46] D. Aloni, Y. Soreq, and M. Williams, *Coupling QCD-Scale Axionlike Particles to Gluons*, *Phys. Rev. Lett.* **123** (2019), no. 3 031803, [`arXiv:1811.03474`].

[47] S. Chakraborty, M. Kraus, V. Loladze, T. Okui, and K. Tobioka, *Heavy QCD axion in b→s transition: Enhanced limits and projections*, *Phys. Rev. D* **104** (2021), no. 5 055036, [`arXiv:2102.04474`].

[48] J. Alwall, R. Frederix, S. Frixione, V. Hirschi, F. Maltoni, O. Mattelaer, H. S. Shao, T. Stelzer, P. Torrielli, and M. Zaro, *The automated computation of tree-level and*

next-to-leading order differential cross sections, and their matching to parton shower simulations, *JHEP* **07** (2014) 079, [`arXiv:1405.0301`].

[49] A. Alloul, N. D. Christensen, C. Degrande, C. Duhr, and B. Fuks, *FeynRules 2.0 - A complete toolbox for tree-level phenomenology*, *Comput. Phys. Commun.* **185** (2014) 2250–2300, [`arXiv:1310.1921`].

[50] C. Degrande, C. Duhr, B. Fuks, D. Grellscheid, O. Mattelaer, and T. Reiter, *UFO - The Universal FeynRules Output*, *Comput. Phys. Commun.* **183** (2012) 1201–1214, [`arXiv:1108.2040`].

[51] T. Sjöstrand, S. Ask, J. R. Christiansen, R. Corke, N. Desai, P. Ilten, S. Mrenna, S. Prestel, C. O. Rasmussen, and P. Z. Skands, *An introduction to PYTHIA 8.2*, *Comput. Phys. Commun.* **191** (2015) 159–177, [`arXiv:1410.3012`].

[52] J. Carvalho, *Compilation of cross sections for proton nucleus interactions at the HERA energy*, *Nucl. Phys. A* **725** (2003) 269–275.

[53] V. Shtabovenko, R. Mertig, and F. Orellana, *FeynCalc 9.3: New features and improvements*, *Comput. Phys. Commun.* **256** (2020) 107478, [`arXiv:2001.04407`].

[54] **SHiP** Collaboration, C. Ahdida, R. Albanese, A. Alexandrov, et al., *SHiP Experiment - Progress Report*, tech. rep., CERN, Geneva, 2019.

[55] I. Boiarska, K. Bondarenko, A. Boyarsky, S. Eijima, M. Ovchynnikov, O. Ruchayskiy, and I. Timiryasov, *Probing baryon asymmetry of the Universe at LHC and SHiP*, `arXiv:1902.04535`.

[56] D. Gorbunov, E. Kriukova, and O. Teryaev, *Scalar decay into pions via Higgs portal*, `arXiv:2303.12847`.

[57] J. L. Feng, I. Galon, F. Kling, and S. Trojanowski, *Dark Higgs bosons at the ForwArd Search ExpeRiment*, *Phys. Rev. D* **97** (2018), no. 5 055034, [`arXiv:1710.09387`].

[58] F. Bezrukov and D. Gorbunov, *Light inflaton Hunter's Guide*, *JHEP* **05** (2010) 010, [`arXiv:0912.0390`].

[59] C. Antel et al., *Feebly Interacting Particles: FIPs 2022 workshop report*, `arXiv:2305.01715`.

[60] T. Pierog, I. Karpenko, J. M. Katzy, E. Yatsenko, and K. Werner, *EPOS LHC: Test of collective hadronization with data measured at the CERN Large Hadron Collider*, *Phys. Rev. C* **92** (2015), no. 3 034906, [`arXiv:1306.0121`].

[61] A. Berlin and F. Kling, *Inelastic Dark Matter at the LHC Lifetime Frontier: ATLAS, CMS, LHCb, CODEX-b, FASER, and MATHUSLA*, *Phys. Rev. D* **99** (2019), no. 1 015021, [`arXiv:1810.01879`].

[62] J. Bezanson, A. Edelman, S. Karpinski, and V. B. Shah, *Julia: A fresh approach to numerical computing*, *SIAM Review* **59** (2017), no. 1 65–98, [`https://doi.org/10.1137/141000671`].

[63] D. Bachrathy and G. Stépán, *Bisection method in higher dimensions and the*

efficiency number, Periodica Polytechnica Mechanical Engineering **56** (2012), no. 2 81–86.